JPET Fast Forward. Published on September 7, 2018 as DOI: 10.1124/jpet.118.250431
This article has not been copyedited and formatted. The final version may differ from this version.

JPET#250431

Nucleos(t)ide analogs do not independently influence hepatic fibrosis and portal hypertension beyond viral suppression in CBDL-induced cirrhotic rat

Yu-Hsin Hsieh*, Hui-Chun Huang*, Ching-Chih Chang, Chiao-Lin Chuang, Fa-Yauh Lee, Shao-Jung Hsu, Yi-Hsiang Huang, Ming-Chih Hou, Shou-Dong Lee

Division of Gastroenterology and Hepatology, Department of Medicine, Taipei Veterans General Hospital, Taipei, Taiwan (YH Hsieh, HCH, FYL, SJH, YH Huang, MCH); Division of General Medicine, Department of Medicine, Taipei Veterans General Hospital, Taipei, Taiwan (YH Hsieh, HCH, CCC, CLC); Faculty of Medicine, National Yang-Ming University School of Medicine, Taipei, Taiwan (HCH, CCC, CLC, FYL, SJH, YH Huang, MCH, SDL); and Division of Gastroenterology, Department of Medicine, Cheng Hsin General Hospital, Taipei, Taiwan (SDL)

*Yu-Hsin Hsieh and Hui-Chun Huang contributed equally to this study.

Running title: Nucleos(t)ide analogs and non-viral cirrhosis

Correspondence:

Shao-Jung Hsu, M.D., Ph. D.,

Division of Gastroenterology and Hepatology, Department of Medicine, Taipei Veterans General Hospital, No. 201, Sec. 2, Shih-Pai Road, Taipei 112, Taiwan.

Tel: +886-2-28712121 ext. 2014

Fax: + 886-2-2873-9318

Email: sjhsu@vghtpe.gov.tw

Text pages: 15

Tables: 1

Figures: 5

References: 36

Word count of Abstract: 229

Word count of Introduction: 373

Word count of Discussion: 819

Abbreviations:

ALT, alanine aminotransferase; AST, aspartate aminotransferase; BW, body weight; CBDL, common bile duct ligation; CI, cardiac index; CO, cardiac output; DW, distilled water; eNOS, endothelial NO synthase; HBV, hepatitis B virus; HR, heart rate; iNOS, inducible NO synthase; MAP, mean arterial pressure; NUCs, nucleos(t)ide analogs; PP, portal pressure; SMA, superior mesenteric artery; SVR, systemic vascular resistance; TNF-α, tumor necrosis factor (TNF)-α; VEGF, vascular endothelial growth factor; VEGFR2, VEGF receptor 2

Recommended section assignment:

Gastrointestinal, Hepatic, Pulmonary, and Renal

Abstract

Chronic hepatitis is the major cause of liver cirrhosis and portal hypertension. Several factors affect portal pressure, including liver fibrosis, splanchnic vasodilatation and pathological angiogenesis. Nucleos(t)ide analogs (NUCs), the oral antiviral agents, effectively attenuate chronic hepatitis B-related liver cirrhosis and portal hypertension via viral suppression and alleviation of hepatitis. On the other hand, NUCs affect TNF-α, vascular endothelial growth factor (VEGF) and nitric oxide (NO), which participate in fibrogenesis, vasodilatation and angiogenesis. However, whether NUCs independently influence liver fibrosis and portal hypertension beyond viral suppression is unknown. This study thus aimed to evaluate the influences of three frequently used NUCs in rats with non-viral cirrhosis. Male Sprague-Dawley rats received common bile duct ligation (CBDL) to induce cholestatic cirrhosis and portal hypertension. The rats were randomly allocated into four groups, treated per oral with lamivudine (30 mg/kg/day), entecavir (0.09 mg/kg/day), tenofovir (50 mg/kg/day) or distilled water (vehicle control) since the 15th day after CBDL. On the 29th day, liver cirrhosis and portal hypertension-related parameters were evaluated. The results showed that chronic NUCs treatment did not affect hemodynamic parameters, plasma TNF-α concentration, and hepatic fibrogenesis protein expressions in rats with non-viral cirrhosis. Though the mesenteric VEGF receptor 2 phosphorylation was down-regulated in NUCs-treated groups, the splanchnic angiogenesis was not influenced. In conclusion, lamivudine, entecavir and tenofovir had no additional effects on liver cirrhosis and portal hypertension in rats with non-viral cirrhosis.

Introduction

Repetitive liver injury, including chronic viral hepatitis, results in liver cirrhosis. During the progression of cirrhosis, portal hypertension and relevant complications develop. Portal hypertension is attributed to several factors, including liver fibrosis and enhanced vascular tone (McConnell and Iwakiri, 2018). On the other hand, splanchnic inflow increases because of abnormal vasodilatation and angiogenesis attributed mainly to nitric oxide (NO) and vascular endothelial growth factor (VEGF) (Mejias et al., 2009; Sumanovski et al., 1999). As a result, the blood flow towards the portal system increases but the outflow is hindered, which leads to elevated portal pressure. To shunt the abnormal blood flow, portosystemic collateral vessels develop. However, portosystemic collaterals bring lethal complications such as varices bleeding and hepatic encephalopathy. Mitigation of portal hypertension is therefore considered pivotal to improve cirrhotic patients' prognosis. However, currently, the treatment efficacy of pharmacological agents is still suboptimal (Sola et al., 2010).

Nucleos(t)ide analogues (NUCs) serve mainly as reverse transcriptase inhibitors, which block hepatitis B virus (HBV) from multiplying and therefore reduce the amount of viruses. Among NUCs, lamivudine is a nucleoside analogue of cytidine, entecavir is a deoxyguanosine analogue (Sims and Woodland, 2006), and tenofovir is a defective adenosine nucleotide analogue (Perry and Simpson, 2009). These drugs effectively suppress the reverse transcription of HBV and attenuate hepatitis. Long-term treatment with these agents even reverses liver cirrhosis caused by chronic hepatitis B (Chang et al., 2010; Dienstag et al., 2003; Marcellin et al., 2013). Theoretically, the resolution of cirrhosis is caused by suppression of viral activity and subsequent amelioration of inflammation. However, recent studies revealed that these NUCs modulated tumor necrosis factor-α (TNF-α) expression (Biswas et al., 2014; Zidek et al., 1999), NO production (Kostecka et al., 2012; Zidek et al., 2000), and neovascularization (Mizutani et al., 2015), all of them participated in pathogenesis

of liver cirrhosis and portal hypertension. If NUCs exert independent benefits in reversing liver fibrosis and portal hypertension, it is possible that they may be applied to patients with non-viral chronic liver diseases. However, direct effects of NUCs on cirrhosis and portal hypertension without HBV infection have not been surveyed.

This study, therefore, aimed to investigate whether the three most prescribed NUCs used to treat chronic hepatitis B ameliorated fibrogenesis and hemodynamic derangements independent of their anti-viral activity in rats with non-viral cirrhosis.

Material and methods

Animals

Male Sprague-Dawley rats were applied. Liver cirrhosis was induced by common bile duct ligation (CBDL) as previously described (Cameron and Muzaffar Hasan, 1958). Briefly, 270-300 g rats were anaesthetized with 100 mg/kg ketamine via intramuscular injection and were then received a midline abdominal incision. The bile duct was dissected, doubly ligated and transected between the two ligatures. Weekly vitamin K injections (50 μg/kg intramuscularly) were administrated to CBDL rat to reduce the mortality caused by coagulopathy (Kountouras et al., 1984).

All animal experiments were conducted in agreement with Institutional Animal Care and Use Committee (IACUC) of Taipei Veterans General Hospital under the approval number of 2016-096. All animals were maintained with humane care in accordance with the principles described in the "Guide for the Care and Use of Laboratory Animals" organized by the National Academy of Sciences and issued by the National Institutes of Health (NIH publication 86-23 revised 1985).

Experiment design

To investigate the roles of NUCs in non-viral cirrhosis and portal hypertension, rats were randomly allocated into four treatment groups: 1. control (distilled water, vehicle); 2. lamivudine (30 mg/kg/day, p.o.); 3. entecavir (0.09 mg/kg/day, p.o.); 4. tenofovir (50 mg/kg/day, p.o.). The treatment started on the 15th day after CBDL surgery. The dosages were determined according to the previous literature, which were suggested to exert pharmaceutical effects in rats (Li et al., 2013; Lu et al., 2014;

Nirogi et al., 2012). On the 29th day after operations, cirrhosis and portal hypertension-related parameters were determined.

Measurement of systemic and portal hemodynamics

For the measurement of mean arterial pressure (MAP) and heart rate (Salerno et al.), the right carotid artery was cannulated with a PE-50 catheter. For the assessment of portal pressure (PP), the abdomen was opened with a mid-line incision, and the mesenteric vein was cannulated with an 18G cannula. The catheters were connected to a two-channel recorder (MP45, BIOPAC Systems, Goleta, CA, U.S.A.) that converted the input signals into continuous graphs of MAP, HR, and PP. Values of MAP, HR, and PP were recorded when the signals achieved stable state (Huang et al., 2012). Superior mesenteric artery was identified at its aortic origin and a 5-mm segment was gently dissected free from the surrounding tissue. The SMA flow was measured by a pulsed-Doppler flow transducer (TS420, Transonic system Inc., Ithaca, NY, USA). Hepatic inflow (portal part) was measured by flow transducer with an adequate size. The measurement point was as proximal to the liver as possible.

Thermodilution method was applied to obtain Cardiac output (CO), as previously described (Albillos et al., 1992). Briefly, a thermistor was positioned in the aortic arch distal to the aortic valve, and five thermal indicators (100 μL of iced normal saline)

was injected sequentially into the right atrium through a PE-50 catheter. A thermodilution curve was developed after each injection, respectively. The aortic thermistor was connected to a cardiac output computer Cardiomax III (Columbus Instruments International Co., OH, USA). The value of cardiac output was determined as an arithmetic mean of five cardiac output values calculated form thermodilution curves.

Cardiac index (CI, ml/min/100g BW) was defined as CO per 100 g BW. Systemic vascular resistance (SVR, mmHg/ml/min/100 g BW) was determined as CI divided by MAP. Hepatic vascular resistance (HVR, mmHg/ml/min/100 g BW) was calculated as PP divided by hepatic vascular flow (portal part) per 100 g BW. SMA resistance (mmHg/ml/min/100 g BW) was determined as (MAP-PP)/SMA flow per 100 g BW.

Immunofluorescent study for the mesenteric vascular density

Through CD31 immunofluorescence staining, CD31-labelled microvascular networks in rat mesenteric connective tissue windows were quantified to evaluate the occurrence of mesenteric angiogenesis according to the previous study (Huang et al., 2012). Mesenteric windows (wedge-shaped regions of transparent connective tissue bordered by the intestinal wall and the ileal blood vessel pairs) were dissected, washed in phosphate-buffered saline (PBS) and dried on gelatin slides. The mesenteric

windows were fixed in methanol at -20 ℃ for 30 min and then acetone at -20 ℃ for 10 min. Slides were then incubated with mouse anti-rat CD31-biotin (Bio-Rad, Hercules, CA, U.S.A.) at 4 ℃ overnight. After PBS wash, slides were incubated with CY2-conjugated streptavidin (Jackson ImmunoResearch, West Grove, PA, U.S.A.) at room temperature for 1 hr. At least four (×100)-magnification immunofluorescent images were obtained for each mesenteric window using an upright fluorescent microscope (AX80, Olympus, Japan). Images were then thresholded and quantified by Image J software (available for download from the National Institutes of Health (http://rsb.info.nih.gov/ij/)).

Hepatic fibrosis determination with Sirius red staining

Paraffin sections of liver were stained using Sirius red staining kit (Polysciences Inc., Warrington, PA, U.S.A.). The percentage of Sirius red-stained area was quantified by Image J. Briefly, the collagen stained in red was highlighted using color-thresholding function. The percentage of Sirius red-stained area was defined as measured thresholded area per image.

Western blot

Microfuge tubes containing protein extraction solution was spun at 10,000 g for 10 min (4 °C). The supernatants were collected and protein concentrations were

determined by a protein assay kit (Bio-Rad, Hercules, CA, U.S.A.). 100 μg tissue lysates were mixed with 4X SDS loading dye to a final concentration of 2 μg/μL. 20 μg protein samples were subjected to SDS-PAGE and transferred to a PVDF membrane (Bio-Rad). The membranes were incubated with blocking solution (3% bovine serum albumin) at room temperature for 1 hour, and then incubated with primary antibody at 4 °C overnight: anti-VEGF rabbit monoclonal antibody (Millipore, Temecula, CA, U.S.A.); anti-VEGFR2, p-VEGFR2, endothelial nitric oxide synthase (eNOS), p-eNOS, Extracellular signal–regulated kinases (Erk) and p-Erk rabbit monoclonal antibody (Cell signaling, Danvers, MA, U.S.A.); anti-α-smooth muscle actin (α-SMA) and tissue inhibitor of metalloproteinase (TIMP) 1 rabbit monoclonal antibody (Abcam, Cambridge, UK); matrix metalloproteinase (MMP) 13 and β-actin rabbit monoclonal antibody (GeneTex Inc., Irvine, CA, U.S.A.). β-actin served as loading control. The membrane was washed 3 times with TBS-T and then incubated with HRP-conjugated secondary antibody at room temperature for 1 hour. Membranes were washed with TBS-T and developed with the enhanced chemiluminescence (Immobilon Western Chemiluminescent HRP Substrate, Merk Millipore Co., Billerica, MA, USA). The immunoreactive bands of specific proteins were detected by a digital luminescence imaging system (BioSpectrum ® 600 Imaging System, Ultra-Violet Products Ltd., Upland, CA, USA). The signal intensity

(integral volume) of the appropriate band was analyzed and quantified through Image J.

Determination of serum TNF-α level

The plasma TNF-α levels were measured using a commercial enzyme-linked immunoabsorbent assay kit (R&D Systems Inc., MN, U. S. A.) according to the manufacturer's instructions.

Drugs

Lamivudine was purchased from Glaxo Group Ltd. (Brentford, Middlesex, U.K.). Entecavir was purchased from Bristol-Myers Squibb (New York, NY, U.S.A.). Tenofovir was purchased from Gilead science Inc. (Foster city, CA, U.S.A.). All the solutions were prepared freshly on the days of experiments.

Statistical analysis

All results are expressed as mean ± S.E.M. Statistical analyses were performed using an independent *t*-test, one-way ANOVA or repeated-measures ANOVA as appropriate using SPSS 21 for Windows (SPSS Inc., Chicago, IL, U.S.A.). Tukey HSD was applied

for post-hoc test. Results were considered statistically significant at a two-tailed *p*-value less than 0.05.

Results

Systemic effects of NUCs in non-viral cirrhotic rats

As shown in Table 1, there was no significant difference in systemic and portal hemodynamic parameters, including MAP, HR, CI, PP, SVR and SMA resistance, among control, lamivudine, entecavir and tenofovir groups. In short, the NUCs did not affect portal hypertension-related hemodynamic derangements in cirrhotic rats.

Effects of NUCs on hepatic fibrosis in non-viral cirrhotic rats

The extent of hepatic fibrosis, evaluated by Sirius red staining, was not significantly different among NUCs and control groups (Figure 1). The plasma TNF-α level, one of the cytokines that is linked to inflammation, was not significantly different among four groups (Figure 2; control, lamivudine, entecavir, tenofovir (ρg/ml): 23.4±0.85, 28.5±2.86, 32.5±4.83, 25.6±0.42). The plasma liver biochemistry parameters, including AST, ALT and total bilirubin, were not significantly different among the four experimental groups as well (Figure 2). The intrahepatic fibrogenesis-related protein expressions, including TIMP1, MMP13 and α-SMA were not significantly different among the four groups (Figure 3).

Effects of NUCs on angiogenesis in non-viral cirrhotic rats.

The mesenteric window vascular density was evaluated by CD31 immunofluorescence staining (Figure 4). There was no significant difference of CD31-stained area ratio among the four groups (control, lamivudine, entecavir, tenofovir (%): 11.03 ± 1.06, 10.51 ± 2.10, 8.39 ± 0.92, 7.46 ± 1.39). Figure 5 disclosed the mesenteric proangiogenic protein expressions. Compared with the control group, VEGFR2 phosphorylation was significantly down-regulated by NUCs (control, lamivudine, entecavir, tenofovir: phospho-VEGFR2: 0.91±0.05, 0.47±0.06, 0.42±0.07, 0.40±0.09, control vs. lamivudine: p=0.002, control vs. entecavir: p=0.001, control vs. tenofovir: p<0.001). The VEGF expression and Erk phosphorylation were up-regulated in NUCs-treated groups, but the difference was not statistically significant (control, lamivudine, entecavir, tenofovir: VEGF: 0.62±0.16, 1.10±0.08, 1.02±0.24, 1.00±0.28; Erk phosphorylation: 0.97±0.18, 1.47±0.2, 1.28±0.28, 1.3±0.4). There was no significant difference on the phosphorylation of eNOS.

JPET Fast Forward. Published on September 7, 2018 as DOI: 10.1124/jpet.118.250431
This article has not been copyedited and formatted. The final version may differ from this version.

Discussion

In this study, the effects of lamivudine, entecavir and tenofovir on non-viral cirrhosis were evaluated. Emerging data show that liver cirrhosis is no longer an irreversible status (Ismail and Pinzani, 2009). Human studies reveal that lamivudine, entecavir and tenofovir suppress the progression of hepatic fibrosis and even reverse chronic hepatitis B-related liver cirrhosis (Chang et al., 2010; Dienstag et al., 2003; Kweon et al., 2001; Liaw, 2013; Marcellin et al., 2013). It is thought that the NUCs attenuate liver cirrhosis by suppressing HBV-related liver damage. However, NUCs have been known to exert effects other than viral suppression, such as NO production (Kostecka et al., 2012; Zidek et al., 1999) and angiogenesis (Mizutani et al., 2015; Song et al., 2017). This study, therefore, assessed the therapeutic potential of NUCs on non-viral cirrhosis.

In this study, liver cirrhosis was induced by CBDL, a well-established animal model with cholestatic liver injury. Indeed, there are several rat models with liver cirrhosis and portal hypertension, including CCl_4 or thioacetamide (TAA) administration and CBDL (Abraldes et al., 2006). In this study, the CCl_4 and TAA models may not be feasible because both hepatotoxins share at least partly, the same metabolic pathways with the NUCs, especially the cytochrome P450s (Nekvindova et al., 2006; Xie et al., 2012), which could significantly interfere with the results. On the

other hand, the CBDL model induced liver injury by overt bile acid accumulation, which is considered far less interfered with the NUCs metabolism (Jaeschke et al., 2002). As a result, we choose the CBDL model to test the effects of NUCs on liver cirrhosis and portal hypertension.

The overproduced collagen fiber in the liver is the cornerstone of liver cirrhosis. It is well recognized that TNF-α plays an important role in the process (Osawa et al., 2013). Interestingly, an *in vitro* study showed that tenofovir upregulated TNF-α expression in endometrial epithelial cells and fibroblasts (Biswas et al., 2014). Moreover, tenofovir enhanced the production of TNF-α in activated murine peritoneal macrophages in a dose-dependent manner (Zidek et al., 2000). However, in this study, the difference on plasma TNF-α level was not statistically significant among the four groups. Consistently, the expression levels of activated hepatic stellate cells (HSCs) marker α-SMA; TIMP1, the tissue inhibitor of metalloproteinase that promotes liver fibrosis (Yoshiji et al., 2000); and MMP13, the extracellular matrix (ECM) enzyme participating in collagen degradation were comparable among four groups. Overall, as indicated by hepatic Sirius red area ratio, NUCs did not affect the severity of liver fibrosis in non-viral cirrhosis.

Hyperdynamic circulation with increased splanchnic inflow contributes to portal hypertension, which is due to excessive pathological angiogenesis and splanchnic

vasodilatation. The VEGF pathway is involved in the abnormal angiogenesis (Fernandez et al., 2004). Inhibition of VEGFR-2 decreases splanchnic hyperdynamic circulation and portosystemic collaterals in portal hypertensive rats rats (Fernandez et al., 2005). The effect of NUCs on angiogenesis inhibition has been noticed. Lamivudine attenuated laser-induced choroidal neovascularization in mice (Mizutani et al., 2015. A recent study also revealed that lamivudine and tenofovir inhibit VEGFR-2 phosphorylation in VEGF-stimulated human dermal microvascular endothelial cells (Song, 2017 #27). In this study, compatible with the previous studies, the VEGFR-2 phosphorylation was significantly down-regulated in NUCs-treated cirrhotic rats. Interestingly, there was a trend toward upregulation in VEGF expression and Erk phosphorylation in NUCs-treated groups. The possible explanations could be compensatorily upregulated VEGF and Erk in response to decreased VEGFR2 phosphorylation, different experimental setting, disease models, animal species, and/or targeted tissues. Nevertheless, the attenuated VEGFR2 activation indicates that the VEGF-signaling in this step was hampered by NUCs. It is thus inferred that many angiogenesis and anti-angiogenesis pathways might interplay during chronic NUCs treatment that the net result as evident by mesenteric vascular density study was not statistically different among control and NUCs groups.

Excessive NO production during the progress of liver cirrhosis results in

splanchnic vasodilatation (Iwakiri and Groszmann, 2007) and angiogenesis (Sumanovski et al., 1999), which then exacerbate portal hypertension. Tenofovir has been found to stimulate NO production. An *in vitro* study showed that the nitrite (a stable metabolite of NO) concentration increased in rat peritoneal cells after 24 hours of tenofovir incubation (Kostecka et al., 2012). On the other hand, tenofovir applied subcutaneously for 16 days significantly increased serum and urine NO concentrations in female Lewis rats with arthritis (Zidek et al., 1999). In the current study, chronic NUCs treatment did not alter the hepatic eNOS phosphorylation and splanchnic blood inflow. The discrepant results might be due to different experimental designs, administration route and treatment duration of pharmacological agents, tissues under survey, and disease models.

In conclusion, lamivudine, entecavir and tenofovir did not affect hepatic fibrosis and portal hypertension-related derangements in non-viral cirrhosis. Despite mesenteric VEGFR2 phosphorylation was down-regulated by NUCs, extrahepatic angiogenesis was not affected. Since NUCs exert a neutral effect on liver fibrosis and portal hypertension independent of HBV suppression, the clinical implication is that currently there is no evidence to support the use of NUCs beyond patients with chronic hepatitis B.

Author contribution

Participated in research design: H.C. Huang and S.J. Hsu
Executed experiments: Y.H. Hsieh and S.J. Hsu
Supervised research: F.Y. Lee
Writing of the manuscript: Y.H. Hsieh, H.C. Huang and S.J Hsu
Data analysis: C.C. Chang and C.L. Chuang
Literature review: Y.H. Huang, M.C. Hou and S.D. Lee

References

Abraldes, J.G., Pasarin, M., and Garcia-Pagan, J.C. (2006). Animal models of portal hypertension. World J Gastroenterol *12*, 6577-6584.

Albillos, A., Colombato, L.A., and Groszmann, R.J. (1992). Vasodilatation and sodium retention in prehepatic portal hypertension. Gastroenterology *102*, 931-935.

Biswas, N., Rodriguez-Garcia, M., Shen, Z., Crist, S.G., Bodwell, J.E., Fahey, J.V., and Wira, C.R. (2014). Effects of tenofovir on cytokines and nucleotidases in HIV-1 target cells and the mucosal tissue environment in the female reproductive tract. Antimicrob Agents Chemother *58*, 6444-6453.

Cameron, G.R., and Muzaffar Hasan, S. (1958). Disturbances of structure and function in the liver as the result of biliary obstruction. J Pathol Bacteriol *75*, 333-349.

Chang, T.T., Liaw, Y.F., Wu, S.S., Schiff, E., Han, K.H., Lai, C.L., Safadi, R., Lee, S.S., Halota, W., Goodman, Z.*, et al.* (2010). Long-term entecavir therapy results in the reversal of fibrosis/cirrhosis and continued histological improvement in patients with chronic hepatitis B. Hepatology *52*, 886-893.

Dienstag, J.L., Goldin, R.D., Heathcote, E.J., Hann, H.W., Woessner, M., Stephenson, S.L., Gardner, S., Gray, D.F., and Schiff, E.R. (2003). Histological outcome during long-term lamivudine therapy. Gastroenterology *124*, 105-117.

Fernandez, M., Mejias, M., Angermayr, B., Garcia-Pagan, J.C., Rodes, J., and Bosch, J. (2005). Inhibition of VEGF receptor-2 decreases the development of hyperdynamic splanchnic circulation and portal-systemic collateral vessels in portal hypertensive rats. J Hepatol *43*, 98-103.

Fernandez, M., Vizzutti, F., Garcia-Pagan, J.C., Rodes, J., and Bosch, J. (2004). Anti-VEGF receptor-2 monoclonal antibody prevents portal-systemic collateral vessel formation in portal hypertensive mice. Gastroenterology *126*, 886-894.

Huang, H.C., Wang, S.S., Hsin, I.F., Chang, C.C., Lee, F.Y., Lin, H.C., Chuang, C.L., Lee, J.Y., Hsieh, H.G., and Lee, S.D. (2012). Cannabinoid receptor 2 agonist ameliorates mesenteric angiogenesis and portosystemic collaterals in cirrhotic rats. Hepatology *56*, 248-258.

Ismail, M.H., and Pinzani, M. (2009). Reversal of liver fibrosis. Saudi J Gastroenterol *15*, 72-79.

Iwakiri, Y., and Groszmann, R.J. (2007). Vascular endothelial dysfunction in cirrhosis. J Hepatol *46*, 927-934.

Jaeschke, H., Gores, G.J., Cederbaum, A.I., Hinson, J.A., Pessayre, D., and Lemasters, J.J. (2002). Mechanisms of hepatotoxicity. Toxicol Sci *65*, 166-176.

Kostecka, P., Holy, A., Farghali, H., Zidek, Z., and Kmonickova, E. (2012). Differential effects of acyclic nucleoside phosphonates on nitric oxide and cytokines in rat hepatocytes and macrophages. Int Immunopharmacol *12*, 342-349.

Kountouras, J., Billing, B.H., and Scheuer, P.J. (1984). Prolonged bile duct obstruction: a new experimental model for cirrhosis in the rat. Br J Exp Pathol *65*, 305-311.

Kweon, Y.O., Goodman, Z.D., Dienstag, J.L., Schiff, E.R., Brown, N.A., Burchardt, E., Schoonhoven, R., Brenner, D.A., and Fried, M.W. (2001). Decreasing fibrogenesis: an immunohistochemical study of paired liver biopsies following lamivudine therapy for chronic hepatitis B. J Hepatol *35*, 749-755.

Li, F.Y., Hao, H.P., Hao, K., Yan, T.T., and Wang, G.J. (2013). Effect of diammonium glycyrrhizinate on entecavir pharmacokinetics in rats. Chin J Nat Med *11*, 309-313.
Liaw, Y.F. (2013). Reversal of cirrhosis: an achievable goal of hepatitis B antiviral therapy. J Hepatol *59*, 880-881.

Liaw, Y.F. (2013). Reversal of cirrhosis: an achievable goal of hepatitis B antiviral therapy. J Hepatol *59*, 880-881.

Lu, C.M., Hou, M.L., Lin, L.C., and Tsai, T.H. (2014). Development of a microdialysis system to monitor lamivudine in blood and liver for the pharmacokinetic application in herbal drug interaction and the gene expression in rats. J Pharm Biomed Anal *96*, 231-240.

Marcellin, P., Gane, E., Buti, M., Afdhal, N., Sievert, W., Jacobson, I.M., Washington, M.K., Germanidis, G., Flaherty, J.F., Aguilar Schall, R.*, et al.* (2013). Regression of cirrhosis during treatment with tenofovir disoproxil fumarate for chronic hepatitis B: a

5-year open-label follow-up study. Lancet *381*, 468-475.

McConnell, M., and Iwakiri, Y. (2018). Biology of portal hypertension. Hepatol Int *12*, 11-23.

Mejias, M., Garcia-Pras, E., Tiani, C., Miquel, R., Bosch, J., and Fernandez, M. (2009). Beneficial effects of sorafenib on splanchnic, intrahepatic, and portocollateral circulations in portal hypertensive and cirrhotic rats. Hepatology *49*, 1245-1256.

Mizutani, T., Fowler, B.J., Kim, Y., Yasuma, R., Krueger, L.A., Gelfand, B.D., and Ambati, J. (2015). Nucleoside Reverse Transcriptase Inhibitors Suppress Laser-Induced Choroidal Neovascularization in Mice. Invest Ophthalmol Vis Sci *56*, 7122-7129.

Nekvindova, J., Masek, V., Veinlichova, A., Anzenbacherova, E., Anzenbacher, P., Zidek, Z., and Holy, A. (2006). Inhibition of human liver microsomal cytochrome P450 activities by adefovir and tenofovir. Xenobiotica *36*, 1165-1177.

Nirogi, R., Bhyrapuneni, G., Kandikere, V., Muddana, N., Saralaya, R., Komarneni, P., Mudigonda, K., and Mukkanti, K. (2012). Pharmacokinetic profiling of efavirenz-emtricitabine-tenofovir fixed dose combination in pregnant and non-pregnant rats. Biopharm Drug Dispos *33*, 265-277.

Osawa, Y., Hoshi, M., Yasuda, I., Saibara, T., Moriwaki, H., and Kozawa, O. (2013). Tumor necrosis factor-alpha promotes cholestasis-induced liver fibrosis in the mouse through tissue inhibitor of metalloproteinase-1 production in hepatic stellate cells. PLoS One *8*, e65251.

Perry, C.M., and Simpson, D. (2009). Tenofovir disoproxil fumarate: in chronic hepatitis B. Drugs *69*, 2245-2256.

Salerno, J.C., Ghosh, D.K., Razdan, R., Helms, K.A., Brown, C.C., McMurry, J.L., Rye, E.A., and Chrestensen, C.A. (2014). Endothelial nitric oxide synthase is regulated by ERK phosphorylation at Ser602. Biosci Rep *34*.

Sims, K.A., and Woodland, A.M. (2006). Entecavir: a new nucleoside analog for the treatment of chronic hepatitis B infection. Pharmacotherapy *26*, 1745-1757.

Sola, E., Lens, S., Guevara, M., Martin-Llahi, M., Fagundes, C., Pereira, G., Pavesi, M., Fernandez, J., Gonzalez-Abraldes, J., Escorsell, A.*, et al.* (2010). Hyponatremia in patients treated with terlipressin for severe gastrointestinal bleeding due to portal hypertension. Hepatology *52*, 1783-1790.

Song, L., Ding, S., Ge, Z., Zhu, X., Qiu, C., Wang, Y., Lai, E., Yang, W., Sun, Y., Chow, S.A.*, et al.* (2017). Nucleoside/nucleotide reverse transcriptase inhibitors attenuate angiogenesis and lymphangiogenesis by impairing receptor tyrosine kinases signalling in endothelial cells. British journal of pharmacology.

Sumanovski, L.T., Battegay, E., Stumm, M., van der Kooij, M., and Sieber, C.C. (1999). Increased angiogenesis in portal hypertensive rats: role of nitric oxide. Hepatology *29*, 1044-1049.

Xie, Y., Wang, G., Wang, H., Yao, X., Jiang, S., Kang, A., Zhou, F., Xie, T., and Hao, H. (2012). Cytochrome P450 dysregulations in thioacetamide-induced liver cirrhosis in rats and the counteracting effects of hepatoprotective agents. Drug Metab Dispos *40*, 796-802.

Yoshiji, H., Kuriyama, S., Miyamoto, Y., Thorgeirsson, U.P., Gomez, D.E., Kawata, M., Yoshii, J., Ikenaka, Y., Noguchi, R., Tsujinoue, H.*, et al.* (2000). Tissue inhibitor of metalloproteinases-1 promotes liver fibrosis development in a transgenic mouse model. Hepatology *32*, 1248-1254.

Zidek, Z., Frankova, D., and Holy, A. (1999). Chemokines, nitric oxide and antiarthritic effects of 9-(2-phosphonomethoxyethyl)adenine (Adefovir). Eur J Pharmacol *376*, 91-100.

Zidek, Z., Frankova, D., and Holy, A. (2000). Macrophage activation by antiviral acyclic nucleoside phosphonates in dependence on priming immune stimuli. Int J Immunopharmacol *22*, 1121-1129.

Footnotes

Yu-Hsin Hsieh and Hui-Chun Huang contributed equally to this study.

Financial support

This study was supported by the grant from Taipei Veterans General Hospital, Taiwan [Grant V106C-077].

Reprint requests to

Shao-Jung Hsu, M.D., Ph. D.,

Division of Gastroenterology and Hepatology, Department of Medicine, Taipei Veterans General Hospital, No. 201, Sec. 2, Shih-Pai Road, Taipei 112, Taiwan.

Email: sjhsu@vghtpe.gov.tw

Figure. 1 Effects of NUCs on hepatic fibrosis area ratio in non-viral cirrhosis. Liver cirrhosis developed 4 weeks after common bile duct ligation (CBDL). Sirius red stained the collagen fiber in red. Compared with distilled water (vehicle)-treated control group, lamivudine, entecavir and tenofovir did not affect hepatic Sirius red staining area ratio. (Number: control, lamivudine, entecavir, tenofovir: 6, 5, 5, 5). Scale bar, 500 μm.

Figure 2. Effects of NUCs on circulating hepatic inflammatory marker in non-viral cirrhosis. TNF-α plays an important role in hepatic inflammation. ALT, AST and total bilirubin represents the severity of liver injury. All of the values were not affected by nucleos(t)ide analogues (NUCs). The results suggested NUCs did not influence non-viral inflammation and the subsequent liver injury.

Figure 3. Effects of NUCs on hepatic fibrogenic protein expression in non-viral cirrhosis. Liver injury activate hepatic stellate cells (HSCs), followed by collagen deposition. The α-SMA is the marker of HSCs activation. TIMP1 and MMP13 participate in hepatic fibrogenesis. All of the proteins were not affected by chronic NUCs administration. (Number: control, lamivudine, entecavir, tenofovir: 5, 5, 5, 5)

Figure 4. Effects of NUCs on mesenteric angiogenesis in non-viral cirrhosis. Mesenteric angiogenesis was determined by vascular density. Chronic NUCs administration did not affect mesenteric vascular density. The representative figures are immunofluorescence staining of endothelial cell marker CD31 in mesenteric windows from CBDL-cirrhotic rats treated with vehicles or NUCs. (Number: control, lamivudine, entecavir, tenofovir: 6, 5, 5, 5). Scale bar, 200 μm.

Figure 5. Effects of NUCs on mesenteric protein expression in non-viral cirrhosis. The mesenteric protein expression of VEGFR2 phosphorylation, VEGF, Erk phosphorylation and eNOS phosphorylation were evaluated by western blots. Compared to control group, NUCs administration significantly down-regulated VEGFR2 phosphorylation. The expression level of VEGF and Erk phosphorylation were upregulated in NUCs treatment groups. eNOS phosphorylation were not affected by NUCs. (Number: control, lamivudine, entecavir, tenofovir: 5, 5, 5, 5) $^{**}p \leq 0.01$, $^{***}p \leq 0.001$ compared with the control group.

JPET Fast Forward. Published on September 7, 2018 as DOI: 10.1124/jpet.118.250431
This article has not been copyedited and formatted. The final version may differ from this version.

Table 1. Hemodynamic parameters in non-viral cirrhotic rats treated with vehicle or NUCs

	Control (n=6)	lamivudine (n=5)	entecavir (n=5)	tenofovir (n=5)
BW (g)	368 ± 20	368 ± 26	381 ± 17	398 ± 14
MAP (mmHg)	94 ± 7	92 ± 3	89 ± 7	100 ± 3
HR (beats/min)	254 ± 22	254 ± 8	246 ± 26	274 ± 6
PP (mmHg)	13.5 ± 0.8	15.6 ± 1.0	13.7 ± 2.7	14.6 ± 1.2
CI (ml/min/100 g)	46 ± 3	48 ± 5	37 ± 4	31 ± 2
SVR (mmHg/ml/min/100 g)	2.1 ± 0.3	2.0 ± 0.2	2.5 ± 0.5	3.2 ± 0.2
SMA flow (ml/min/100 g)	6.2 ± 0.7	7.0 ± 1.0	6.3 ± 0.8	6.1 ± 0.4
SMA resistance (mmHg/ml/min/100 g)	13.8 ± 2.0	11.5 ± 1.3	12.5 ± 1.7	14.2 ± 0..9
Hepatic flow (portal part, ml/min/100 g)	8.2 ± 1.1	10.6 ± 0.9	8.3 ± 1.2	7.9 ± 0.6
HVR (mmHg/ml/min/100 g)	1.8 ± 0.26	1.5 ± 0.1	1.8 ± 0.3	1.9 ± 0.2

CBDL, common bile duct ligation; n, number of rats; control: treated with vehicle as distilled water; BW, body weight; MAP, mean arterial pressure; HR, heart rate; PP, portal pressure; CI, cardiac index; SVR, systemic vascular resistance; SMA, superior mesenteric artery; HVR, hepatic vascular resistance. Values are expressed as mean ± SEM. All $p>0.05$ among groups.

JPET Fast Forward. Published on September 7, 2018 as DOI: 10.1124/jpet.118.250431
This article has not been copyedited and formatted. The final version may differ from this version.

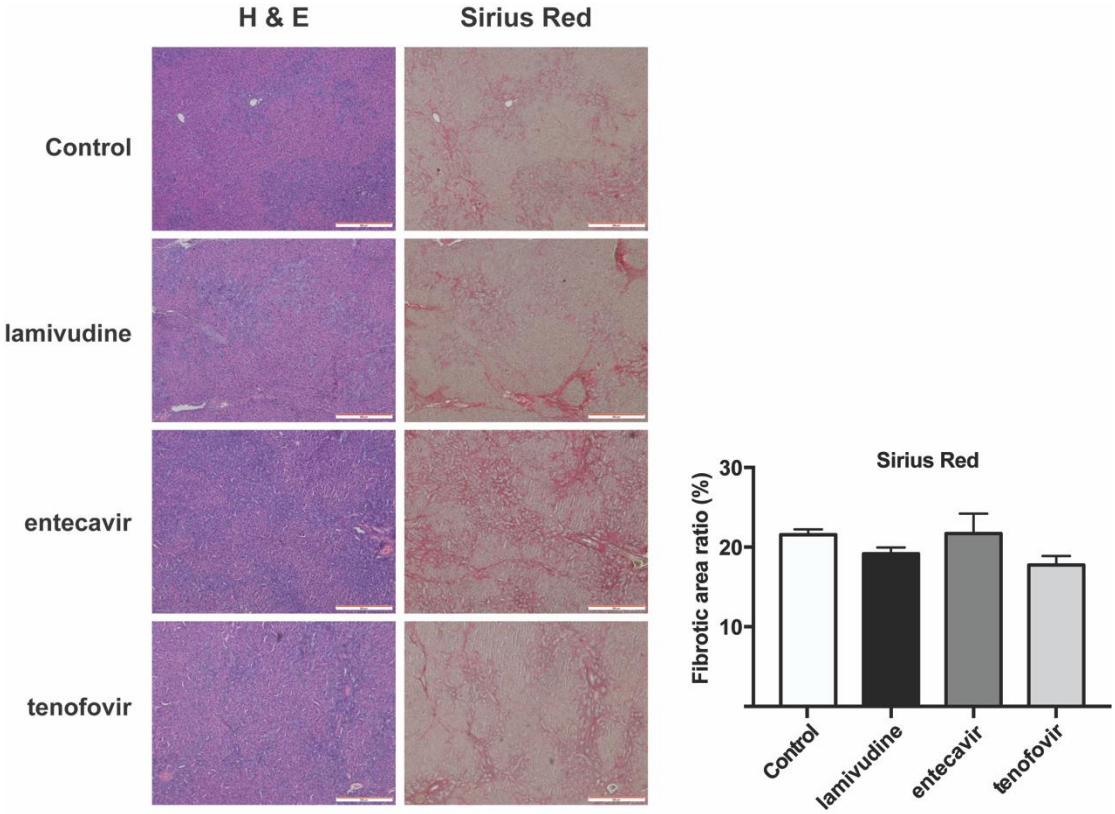

Figure 1

JPET Fast Forward. Published on September 7, 2018 as DOI: 10.1124/jpet.118.250431
This article has not been copyedited and formatted. The final version may differ from this version.

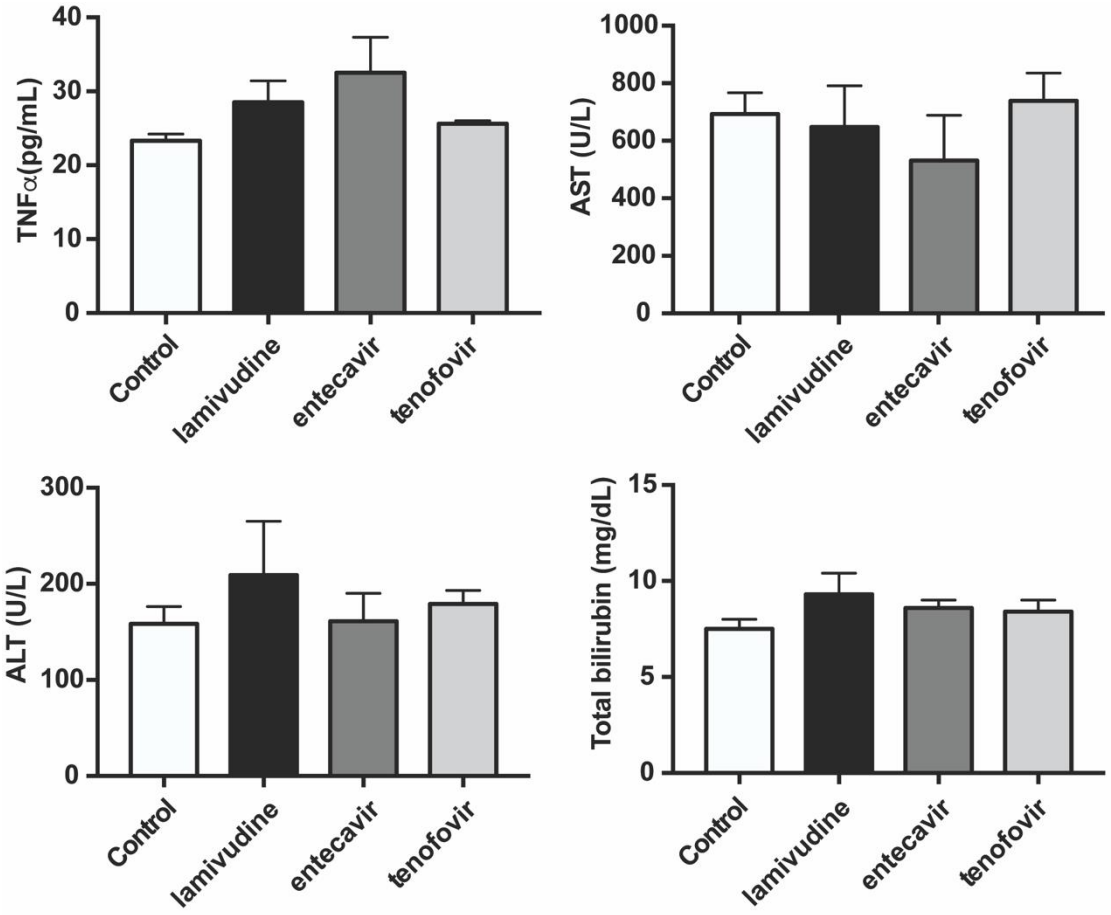

Figure 2

JPET Fast Forward. Published on September 7, 2018 as DOI: 10.1124/jpet.118.250431
This article has not been copyedited and formatted. The final version may differ from this version.

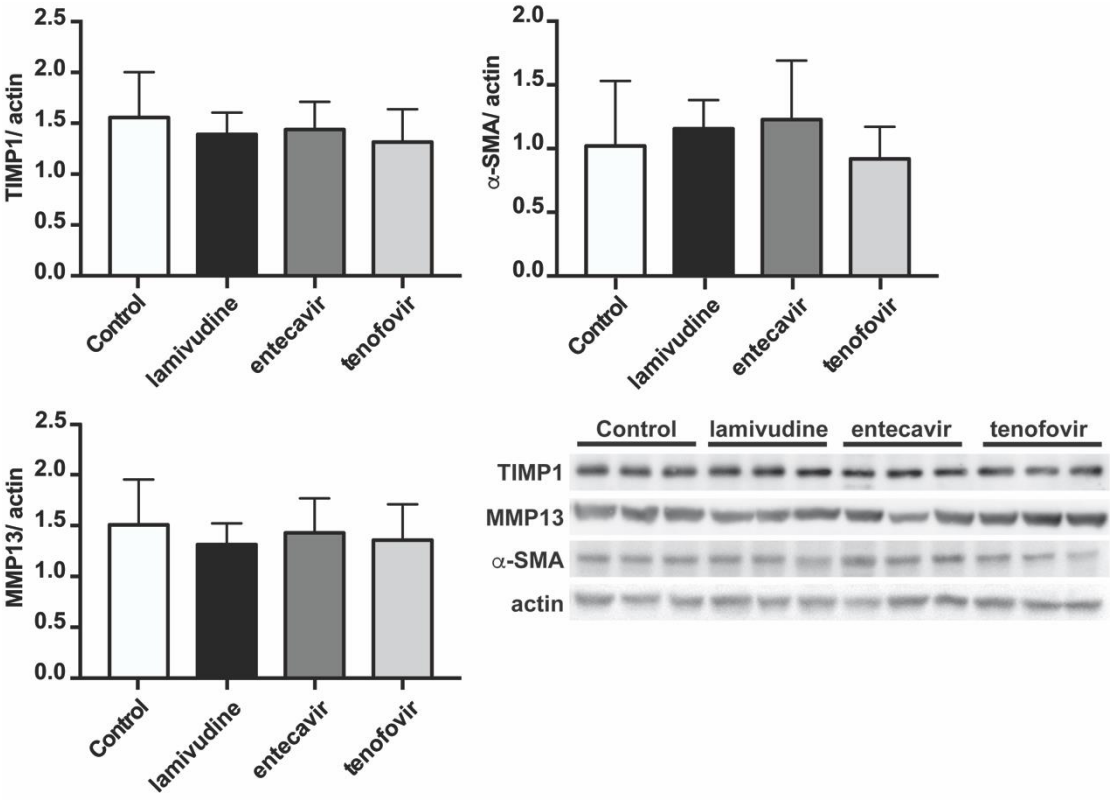

Figure 3

JPET Fast Forward. Published on September 7, 2018 as DOI: 10.1124/jpet.118.250431
This article has not been copyedited and formatted. The final version may differ from this version.

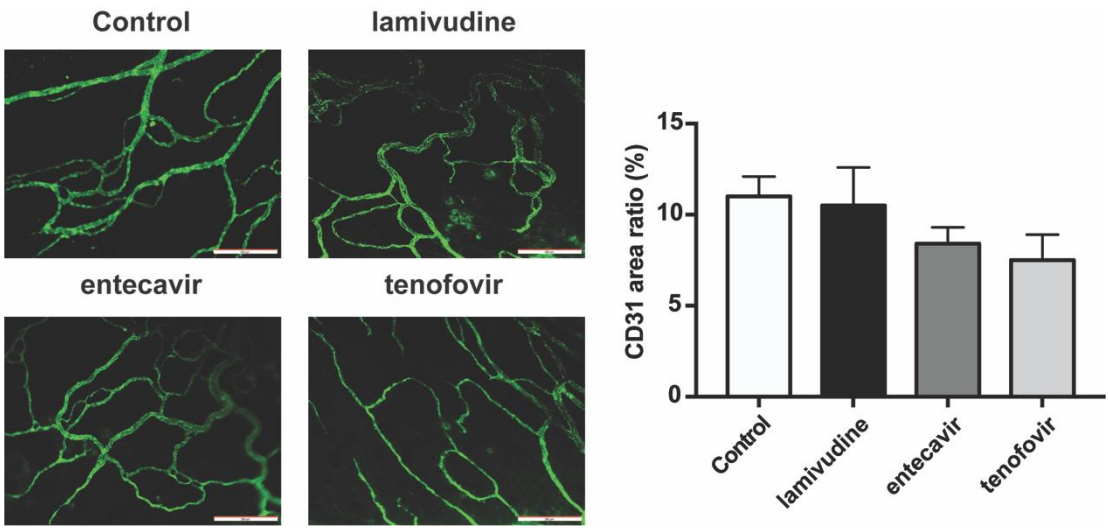

Figure 4

JPET Fast Forward. Published on September 7, 2018 as DOI: 10.1124/jpet.118.250431
This article has not been copyedited and formatted. The final version may differ from this version.

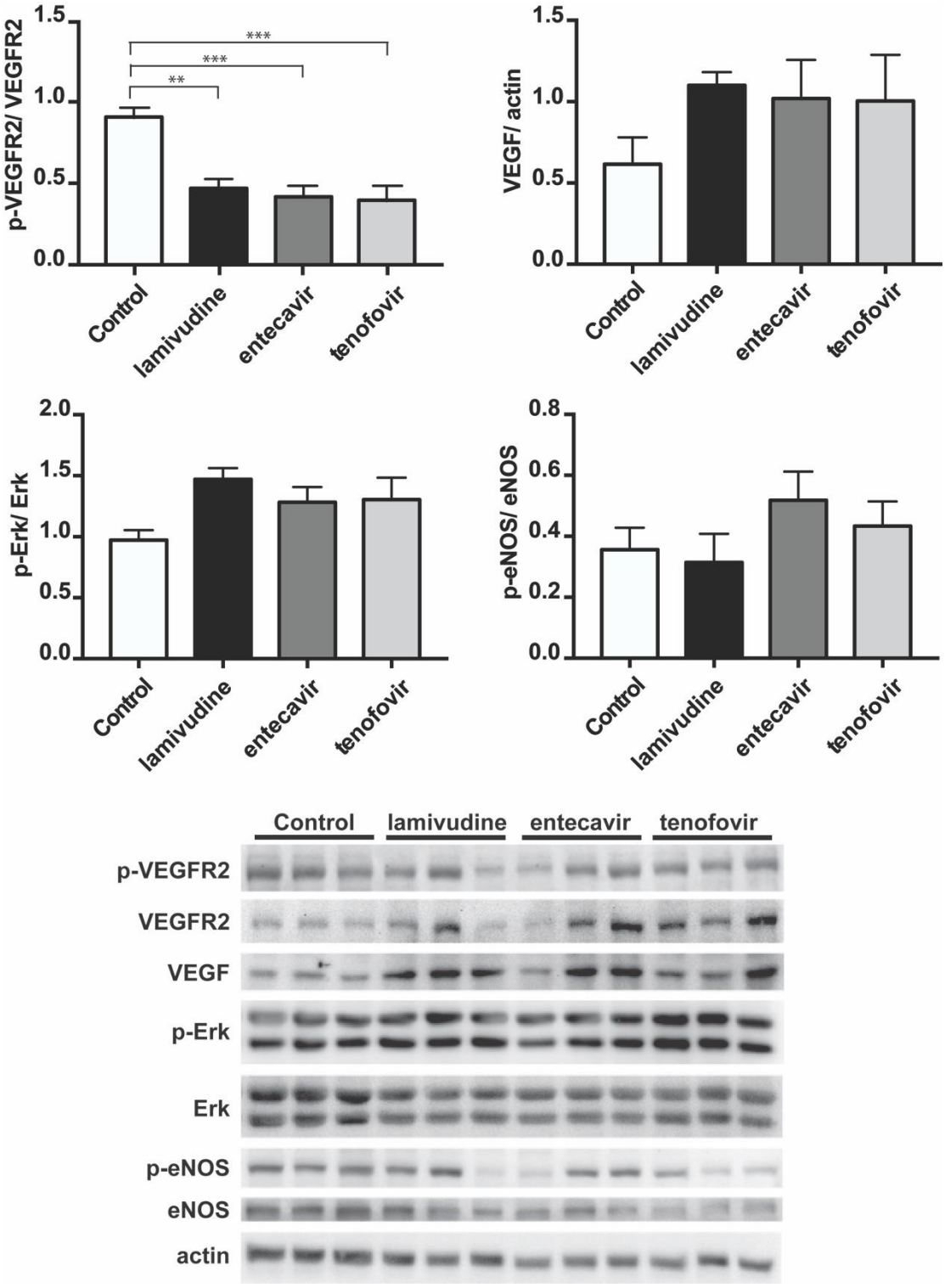

Figure 5